Available online at www.sciencedirect.com
SCIENCE DIRECT
Journal of Molecular Spectroscopy 237 (2006) 87–96
Journal of MOLECULAR SPECTROSCOPY
www.elsevier.com/locate/jms

Multi-isotopologue analyses of new vibration–rotation and pure rotation spectra of ZnH and CdH

Alireza Shayesteh [a], Robert J. Le Roy [a], Thomas D. Varberg [b], Peter F. Bernath [a,*]

[a] Department of Chemistry, University of Waterloo, Waterloo, Ont., Canada N2L 3G1
[b] Department of Chemistry, Macalester College, 1600 Grand Ave., St. Paul, MN 55105, USA

Received 14 February 2006
Available online 10 March 2006

Abstract

High resolution infrared emission spectra of ZnH, ZnD, CdH, and CdD have been recorded with a Fourier transform spectrometer. The $v = 1 \rightarrow 0$ and $v = 2 \rightarrow 1$ bands of ZnH, ZnD, CdH, and CdD, as well as the $v = 3 \rightarrow 2$ band of ZnD were observed for the $X\,^2\Sigma^+$ ground electronic state. In addition, new rotational spectra have been recorded for CdH and CdD using a tunable far-infrared spectrometer, and pure rotational transitions in the $v = 1$ level of the ground state were measured. The new data were combined with the previous data from diode laser infrared spectra and pure rotation spectra of ZnH/ZnD and CdH/CdD available in the literature. The data from all isotopologues were fitted together using a Dunham-type energy level expression for $^2\Sigma^+$ states, and Born–Oppenheimer breakdown correction parameters were obtained. The equilibrium rotational constants (B_e) of ^{64}ZnH, ^{64}ZnD, ^{114}CdH, and ^{114}CdD were determined to be 6.691332(17), 3.402156(7), 5.447074(18), and 2.750761(6) cm^{-1}, respectively, and the associated equilibrium internuclear distances (r_e) are 1.593478(2), 1.593001(2), 1.760098(3), and 1.759695(2) Å, respectively. Simple reduced mass scaling for the spin–rotation interaction constants of ZnH and CdH fully accounted for their isotopologue dependence, and no Born–Oppenheimer breakdown correction was required for these parameters.

Keywords: ZnH; CdH; ZnD; CdD; Vibration–rotation spectra; Pure rotation spectra; Multi-isotopologue fitting; Dunham constants; Born–Oppenheimer breakdown

1. Introduction

Gaseous ZnH_2, CdH_2, and HgH_2 molecules have been discovered recently in our laboratory at the University of Waterloo, and their infrared emission spectra were recorded at high resolution using a Fourier transform spectrometer [1–5]. These spectra also contained a few vibration–rotation bands of ZnH, ZnD, CdH, and CdD in the $X\,^2\Sigma^+$ ground state, which are described in this paper. In addition to these infrared emission spectra, we have recorded new far-infrared spectra of the CdH and CdD molecules. Zinc and cadmium have several naturally abundant isotopes, and high resolution spectra of ZnH, ZnD, CdH, and CdD are valuable for studying small isotope effects due to both metal and hydrogen atoms.

The ZnH and CdH molecules were first observed in the 1920s through their electronic spectra in the visible/near-ultraviolet region [6–12], their identification being primarily based on the large line spacings [7] and the isotope effects [8]. Rotational analyses of the spectra by Mulliken and Hulthén [10–12] resulted in spectroscopic constants for the $X\,^2\Sigma^+$ ground state and the $A\,^2\Pi$ excited state of each species. The Zeeman effect in the A–X band systems of ZnH and CdH was studied by Watson [13]. Further investigations were undertaken in the 1930s, and two electronic transitions, $A\,^2\Pi \rightarrow X\,^2\Sigma^+$ and $B\,^2\Sigma^+ \rightarrow X\,^2\Sigma^+$, were studied in detail [14–22]. The most complete analyses of the A–X and B–X bands of ZnH and CdH were performed by Stenvinkel [17] and Svensson [18], respectively. The 0–0 bands of the $A\,^2\Pi \rightarrow X\,^2\Sigma^+$ transitions of ZnD and

* Corresponding author. Fax: +1 519 746 0435.
E-mail address: bernath@uwaterloo.ca (P.F. Bernath).

0022-2852/$ - see front matter © 2006 Elsevier Inc. All rights reserved.
doi:10.1016/j.jms.2006.03.004

CdD were analyzed by Fujioka and Tanaka [19] and Deile [20], respectively. The absorption spectra of ZnH, ZnD, CdH, and CdD in the far-ultraviolet region were analyzed by Khan [23,24], and a new electronic transition, $C\ ^2\Sigma^+ \leftarrow X\ ^2\Sigma^+$, was assigned for these molecules. Huber and Herzberg [25] compiled a nearly complete summary of the ZnH and CdH studies prior to 1975.

The $A\ ^2\Pi \rightarrow X\ ^2\Sigma^+$ and $B\ ^2\Sigma^+ \rightarrow X\ ^2\Sigma^+$emission spectra of ZnD and CdD were recorded by Balfour and co-workers in the 1980s [26–29], and several vibrational bands were analyzed. The molecules were generated in an arc source, and the spectra were recorded by classical spectrographs. Balfour's data spanned the $v = 0$ to 3 levels of the $X\ ^2\Sigma^+$ ground states of ZnD and CdD. A few years later, O'Brien et al. [30] measured the 0–0 band of the $A\ ^2\Pi \rightarrow X\ ^2\Sigma^+$ system of ZnD at high resolution using a hollow cathode discharge lamp and a Fourier transform spectrometer.

The equilibrium internuclear distances, vibrational frequencies, dissociation energies, and dipole moments of the ZnH and CdH molecules have been computed in several ab initio theoretical studies [31–35]. These calculations further confirmed the experimental assignments of the $A\ ^2\Pi$, $B\ ^2\Sigma^+$, and $C\ ^2\Sigma^+$ states [33–35]. Hyperfine structure, Λ-doubling and lifetimes of ZnH and CdH have been measured by laser-induced fluorescence spectroscopy [36,37] and by matrix-isolation electron spin resonance (MI-ESR) techniques [38–40]. Low resolution infrared absorption spectra of ZnH, ZnD, CdH, and CdD trapped in solid argon, neon, and hydrogen matrices have also been recorded [41,42]. Of astrophysical interest, Wojslaw and Peery [43] claim to have detected some branches of the 0–0 and 1–0 bands of the A–X system of ZnH in the absorption spectrum of the star 19 Piscium.

The only previous high resolution infrared spectra of zinc and cadmium monohydride are those obtained by Jones and co-workers [44,45]. They used a diode-laser infrared spectrometer and observed the $v = 1 \leftarrow 0$ and $v = 2 \leftarrow 1$ bands of ZnH, ZnD, CdH, and CdD in the $X\ ^2\Sigma^+$ ground state. However, the number of rotational lines observed in each band was limited by the spectral ranges of the diodes available. Millimeter-wave and far-infrared spectra of ZnH and ZnD were obtained by Goto et al. [46] and Tezcan et al. [47], respectively, and several rotational lines in the $v = 0$ level of the $X\ ^2\Sigma^+$ ground state were measured. Recently, Varberg and Roberts [48] recorded the far-infrared spectra of CdH and CdD, and observed rotational transitions in the $v = 0$ level of the $X\ ^2\Sigma^+$ ground state. They performed a multi-isotopologue fit to their data, but overlooked the vibrational dependence of the rotational and spin–rotation interaction constants. This resulted in an anomalously large number of correction parameters being attributed to the breakdown of the Born–Oppenheimer approximation.

In this paper we report new Fourier transform infrared emission spectra containing the $v = 1 \rightarrow 0$ and $v = 2 \rightarrow 1$ bands of ZnH, ZnD, CdH, and CdD, as well as the $v = 3 \rightarrow 2$ band of ZnD in the $X\ ^2\Sigma^+$ ground state. In addition, we have recorded new far-infrared spectra of CdH and CdD, and observed several rotational transitions in the $v = 1$ level of the $X\ ^2\Sigma^+$ state. We have combined our new data with those obtained from the previous vibration–rotation and pure rotation spectra [44–48], and performed multi-isotopologue fits for ZnH and CdH using a Dunham-type energy level expression [49] that was modified for $^2\Sigma^+$ states. The isotopic dependence of the spin–rotation interaction constant (γ), derived by Brown and Watson [50], was implemented in our fitting program, and we also included a simple vibrational dependence for this constant. We show that many of the Born–Oppenheimer breakdown correction parameters reported by Varberg and Roberts [48] vanish if the vibrational dependences of rotational and spin–rotation interaction constants are taken into account properly.

2. Experiments

The infrared emission spectra of the ZnH, ZnD, CdH, and CdD molecules were generated using an emission source that combines an electrical discharge with a high temperature furnace. The discharge-furnace setup in our laboratory at the University of Waterloo has been described in detail in previous reports on ZnH_2, CdH_2, and HgH_2 molecules [1–3]. A small tantalum boat containing about 100 g of zinc or cadmium was placed inside the central part of an alumina tube, and heated to 470 or 350 °C, respectively, to produce about 0.5 Torr of metal vapor. The tube was sealed with BaF_2 or KBr windows, and pure hydrogen or deuterium (total pressure ~0.5–2.5 Torr) flowed slowly through the cell. A dc discharge (3 kV, 333 mA) was created between two stainless steel electrodes located inside the water-cooled ends of the alumina tube, and a BaF_2 or KBr lens was used to focus the emission onto the entrance aperture of a Bruker IFS HR 120 Fourier transform spectrometer. Infrared emission spectra were recorded using a KBr beamsplitter and a liquid-nitrogen-cooled HgCdTe (MCT) detector. Infrared longwave-pass filters were used to limit the spectral range to the 1200–2200 cm^{-1} region for ZnH/CdH, and to the 800–1600 cm^{-1} region for ZnD/CdD. The instrumental resolution was set to 0.01 cm^{-1}, and a few hundred spectra were co-added to improve the signal-to-noise ratio. Overall, the emission lines from ZnH and ZnD were nearly four times stronger than those from CdH and CdD.

The far-infrared absorption spectra of CdH and CdD were recorded using the NIST TuFIR spectrometer in Boulder, Colorado, and the experimental conditions were exactly the same as those described in the recent paper of Varberg and Roberts on these molecules [48]. The CdH and CdD molecules were generated in a quartz discharge tube that had seven equally spaced 1-cm-deep depressions in it, into which cadmium metal was placed. The tube was wrapped with heating tape, and the temperature was increased to about 480 °C. Pure hydrogen at 0.4 Torr or a mixture of deuterium and argon at 0.7 Torr flowed slowly

through the tube, and a 100 mA discharge was created between two wire electrodes located near the two ends of the quartz tube. The tunable far-infrared radiation was generated by mixing radiation from two frequency-stabilized CO_2 lasers with a tunable microwave amplifier. The radiation was collimated by a parabolic mirror, passed through the absorption cell, and focused onto a liquid-helium-cooled bolometer or photoconductor. The CdH and CdD spectra were acquired by sinusoidally modulating the frequency of one of the CO_2 lasers at about 1 kHz and by detecting the absorption signal with a lock-in amplifier. Due to the frequency modulation, lines in the far-infrared spectra appeared as first derivatives of the absorption profile.

3. Results and analyses

3.1. Infrared emission spectra

The infrared emission spectra contained atomic and molecular emission lines, as well as blackbody emission from the hot tube and absorption lines from atmospheric water vapor. To obtain flat baselines, the blackbody emission profile was subtracted from the spectra using the Bruker OPUS software. The $v = 1 \rightarrow 0$ and $v = 2 \rightarrow 1$ bands of ZnH, ZnD, CdH, and CdD, as well as the $v = 3 \rightarrow 2$ band of ZnD in the $X\,^2\Sigma^+$ ground state were observed in emission. An overview of the infrared emission spectrum of ZnH is presented in Fig. 1, and the *R*-branch of the $v = 1 \rightarrow 0$ band of ZnD is shown in Fig. 2.

Zinc has five stable isotopes with the following terrestrial abundances: ^{64}Zn (48.6%), ^{66}Zn (27.9%), ^{67}Zn (4.1%), ^{68}Zn (18.8%), and ^{70}Zn (0.6%). The terrestrial abundances for the eight isotopes of cadmium are: ^{106}Cd (1.3%), ^{108}Cd (0.9%), ^{110}Cd (12.5%), ^{111}Cd (12.8%), ^{112}Cd (24.1%), ^{113}Cd (12.2%), ^{114}Cd (28.7%), and ^{116}Cd (7.5%). Lines from most of these isotopes

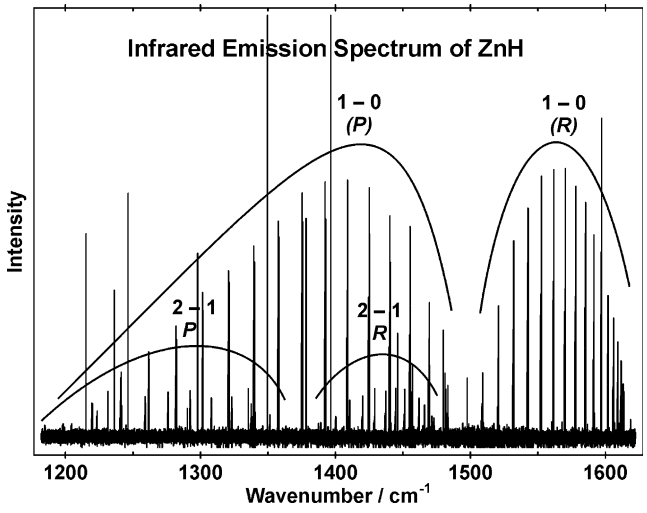

Fig. 1. An overview of the infrared emission spectrum of ZnH recorded at 0.01 cm^{-1} resolution.

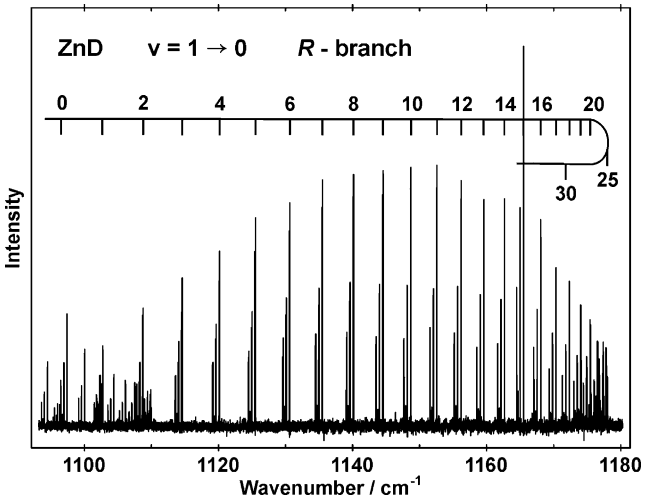

Fig. 2. A portion of the infrared emission spectrum of ZnD showing the *R*-branch head of the fundamental band.

(all except ^{70}Zn, ^{106}Cd, and ^{108}Cd) were observed in our infrared emission spectra, and the isotope splittings were completely resolved. The spin–rotation interaction in $^2\Sigma^+$ states removes the degeneracy of the *e* (F_1) and *f*(F_2) parity components, and we observed a doublet splitting in almost all vibration–rotation lines. The isotope splitting and spin splitting in one rotational line of CdH and ZnD are shown in Figs. 3 and 4, respectively.

Line positions were measured using the WSPECTRA program written by Carleer (Université Libre de Bruxelles). In addition to ZnH, ZnD, CdH, and CdD, molecular emission lines from ZnH_2, ZnD_2, CdH_2, and CdD_2 were observed, and the analyses of their spectra have been published [1–4]. The ZnH and CdH spectra also contained strong CO (impurity) emission lines, which were used for absolute wavenumber calibration [51]. The ZnD and CdD spectra were then calibrated using several atomic

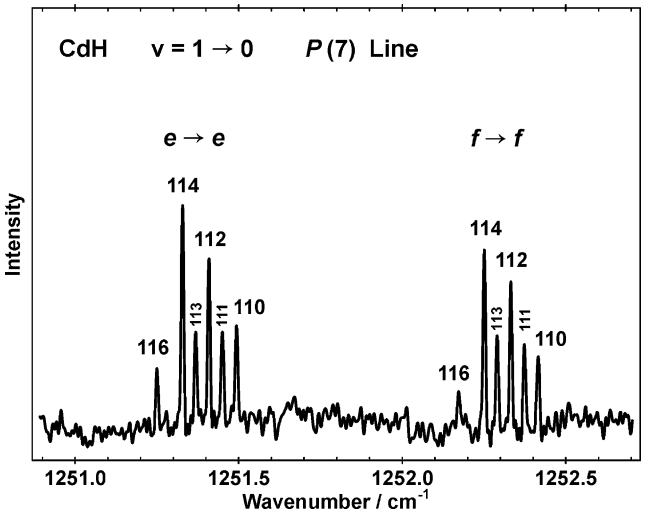

Fig. 3. An expanded view of one rotational line in the CdH infrared spectrum showing the spin doubling (*e*/*f*) and the isotope splitting. Lines have been marked by the mass numbers of cadmium isotopes.

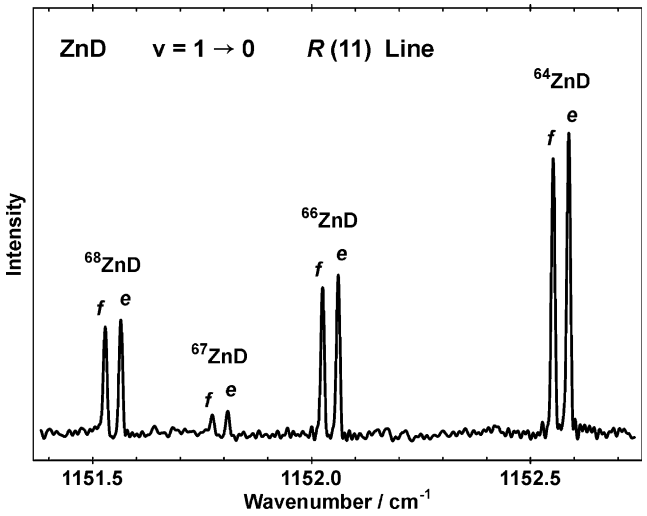

Fig. 4. An expanded view of one rotational line in the ZnD infrared spectrum showing the isotope splitting and the spin doubling (*e*/*f*).

emission lines that were common to both hydride and deuteride spectra. The absolute accuracy of calibrated line positions in ZnH and ZnD spectra is about 0.0005 cm^{-1}. The calibrated CdH and CdD line positions have an accuracy of about 0.001 cm^{-1}.

3.2. Far-infrared absorption spectra

The new far-infrared absorption spectra of cadmium hydride cover several pure rotational lines in the $v = 1$ level of the $X\ ^2\Sigma^+$ ground state. These spectra involve the isotopologues ^{114}CdH, ^{112}CdH, and ^{110}CdH over the range $N'' = 4$ to 11 and ^{116}CdD, ^{114}CdD, ^{112}CdD, and ^{110}CdD over the range $N'' = 9$–20. Magnetic hyperfine structure arising from the ^{1}H or ^{2}D nucleus was present in all these spectra, but was fully resolved only for the lowest-N transitions of CdH. We fitted the hyperfine structure of these low-N rotational lines of CdH in the $v = 1$ level, and found it to be 10% larger than that in the corresponding rotational lines within the $v = 0$ level [48]. This determination allowed us to predict hyperfine splittings over the full range of $v = 1$ rotational levels studied, which is required for an accurate analysis of the observed line shapes, as described in [48].

To properly combine these pure rotational transitions with the infrared rovibrational transitions in the global fit, it was necessary to calculate frequencies of the transitions in the absence of hyperfine structure. We accomplished this by first fitting a parameterized Hamiltonian including rotational, spin–rotation, and hyperfine terms to each isotopologue separately. We then set the hyperfine parameters to be identically zero and used the fitted values of the rotational and spin–rotation constants to calculate the hypothetical "hyperfine-free" positions of the pure rotational lines. These frequencies were subsequently used in the global fit to all of the spectroscopic data. This procedure is more accurate than simply determining a single average frequency in fitting the line shapes of the hyperfine-blended pure rotational transitions, because matrix elements in the hyperfine Hamiltonian that are off-diagonal in J cause small but significant shifts in the rotational levels. We estimated the uncertainties in these "hyperfine-free" pure rotational lines to be 5×10^{-6} cm^{-1} (150 kHz).

3.3. Data analysis

The published diode laser infrared spectra of ZnH, ZnD, CdH, and CdD contained the $v = 1 \leftarrow 0$ and $v = 2 \leftarrow 1$ bands for these species [44,45]. The number of rotational lines in each band was limited, due to spectral gaps in the diodes available. For example, only one rotational line was observed in the *P*-branch of the $v = 2 \leftarrow 1$ bands of ZnD and CdD [44,45]. We included all the diode laser infrared lines in our data set, and there was no systematic discrepancy between those lines and our calibrated line positions. The available pure rotation data [46–48] were also included in our data set as hyperfine-free line positions calculated in the same manner as mentioned above.

The program DParFit [52] was used to obtain conventional band constants by fitting the data to analytic energy level expressions derived from the following Hamiltonian operator:

$$\hat{\mathbf{H}} = B\hat{\mathbf{N}}^2 - D\hat{\mathbf{N}}^4 + H\hat{\mathbf{N}}^6 + L\hat{\mathbf{N}}^8 + \hat{\mathbf{N}} \cdot \hat{\mathbf{S}}\left(\gamma + \gamma_D\hat{\mathbf{N}}^2 + \gamma_H\hat{\mathbf{N}}^4\right). \tag{1}$$

The band constants were sequentially rounded and refitted [53] starting from the highest order parameter of the highest observed vibrational level. The rounded constants for ^{64}ZnH, ^{64}ZnD, ^{114}CdH, and ^{114}CdD are reported in Tables 1 and 2.

The data for all isotopologues were then combined and fitted simultaneously using Dunham-type energy level expressions modified for $^2\Sigma^+$ states, i.e., the following equations for $e(J = N + 1/2)$ and $f(J = N - 1/2)$ parities, respectively.

$$E^e_{v,N} = \sum_{m=0}\sum_{l=0} Y_{l,m}\left(v+\frac{1}{2}\right)^l [N(N+1)]^m + \frac{1}{2}(N)\sum_{m=1}\sum_{l=0}\gamma_{l,m}\left(v+\frac{1}{2}\right)^l [N(N+1)]^{m-1}, \tag{2}$$

$$E^f_{v,N} = \sum_{m=0}\sum_{l=0} Y_{l,m}\left(v+\frac{1}{2}\right)^l [N(N+1)]^m - \frac{1}{2}(N+1)\sum_{m=1}\sum_{l=0}\gamma_{l,m}\left(v+\frac{1}{2}\right)^l [N(N+1)]^{m-1}. \tag{3}$$

In Le Roy's formulation of the Born–Oppenheimer breakdown parameters [54] for a diatomic molecule A–B, the Dunham constants for each isotopologue (α) are related to those for a chosen reference isotopologue ($\alpha = 1$) by the following equation:

Table 1
Band constants (in cm^{-1}) for the $X\,^2\Sigma^+$ ground state of ^{64}ZnH and ^{64}ZnD[a]

Molecule	Constant	$v=0$	$v=1$	$v=2$	$v=3$
^{64}ZnH	G_v	0.0	1496.47788(22)	2873.7218(5)	
	B_v	6.5476308(9)	6.2420626(78)	5.900569(25)	
	$10^4 D_v$	4.72631(14)	4.96334(72)	5.3998(34)	
	$10^9 H_v$	7.08(8)	−1.73(24)	−22.5(16)	
	$10^{12} L_v$	−3.99(14)	−9.8(3)	−21(3)	
	γ_v	0.253108(4)	0.23366(4)	0.21193(8)	
	$10^4 \gamma_{D,v}$	−0.7930(7)	−0.806(2)	−0.868(4)	
	$10^9 \gamma_{H,v}$	5.1(4)	—	—	
^{64}ZnD	G_v	0.0	1089.91437(14)	2122.38807(21)	3092.1493(8)
	B_v	3.35036133(49)	3.2425018(28)	3.127117(5)	3.001227(16)
	$10^4 D_v$	1.21635(3)	1.25213(14)	1.30817(30)	1.3905(7)
	$10^9 H_v$	1.0632(84)	0.364(24)	−0.78(7)	−4.26(9)
	$10^{12} L_v$	−0.225(7)	−0.42(1)	−0.78(5)	—
	γ_v	0.129973(3)	0.123093(18)	0.11579(3)	0.10781(8)
	$10^4 \gamma_{D,v}$	−0.20372(18)	−0.2032(4)	−0.2119(6)	−0.225(2)
	$10^9 \gamma_{H,v}$	0.66(3)	—	—	—

[a] The numbers in parentheses are 2σ uncertainties in the last quoted digits.

Table 2
Band constants (in cm^{-1}) for the $X\,^2\Sigma^+$ ground state of ^{114}CdH and ^{114}CdD[a]

Molecule	Constant	$v=0$	$v=1$	$v=2$
^{114}CdH	G_v	0.0	1336.9576(2)	2549.9724(16)
	B_v	5.3254120(3)	5.0631697(11)	4.76031(7)
	$10^4 D_v$	3.171414(39)	3.4278(2)	3.961(6)
	$10^9 H_v$	−1.265(24)	−10.36(13)	—
	$10^{12} L_v$	−2.65(5)	−6.8(3)	—
	γ_v	0.604595(3)	0.55218(1)	0.4916(4)
	$10^4 \gamma_{D,v}$	−1.71829(29)	−1.8101(5)	−1.99(5)
	$10^9 \gamma_{H,v}$	6.41(9)	—	—
^{114}CdD	G_v	0.0	973.5970(2)	1888.6176(16)
	B_v	2.70739863(20)	2.6165496(30)	2.517426(31)
	$10^4 D_v$	0.80227(2)	0.84119(27)	0.908(1)
	$10^9 H_v$	−0.056(8)	−0.590(96)	—
	$10^{12} L_v$	−0.13(1)	−0.4(1)	—
	γ_v	0.308833(3)	0.290693(24)	0.2707(3)
	$10^4 \gamma_{D,v}$	−0.43525(19)	−0.4474(6)	−0.46(2)
	$10^9 \gamma_{H,v}$	0.91(3)	—	—

[a] The numbers in parentheses are 2σ uncertainties in the last quoted digits.

$$Y_{l,m}^{(\alpha)} = \left\{ Y_{l,m}^{(1)} + \left(\frac{M_A^{(\alpha)} - M_A^{(1)}}{M_A^{(\alpha)}} \right) \delta_{l,m}^{A} + \left(\frac{M_B^{(\alpha)} - M_B^{(1)}}{M_B^{(\alpha)}} \right) \delta_{l,m}^{B} \right\} \left(\frac{\mu_1}{\mu_\alpha} \right)^{m+l/2}. \quad (4)$$

In the above equation, $\delta_{l,m}^{A}$ and $\delta_{l,m}^{B}$ are the Born–Oppenheimer breakdown correction parameters for atoms A and B, respectively, M_A and M_B are atomic masses, and μ's are reduced masses. An analogous reduced mass scaling relationship exists for the spin–rotation interaction constants [50]:

$$\gamma_{l,m}^{(\alpha)} = \gamma_{l,m}^{(1)} \left(\frac{\mu_1}{\mu_\alpha} \right)^{m+l/2}. \quad (5)$$

Program DParFit was used for multi-isotopologue fitting, with the reference isotopologues chosen to be ^{64}ZnH and ^{114}CdH. The Dunham constants of the reference isotopologues and the Born–Oppenheimer breakdown correction parameters are presented in Tables 3 and 4. The sequential rounding and refitting technique [53], starting from the parameter with largest relative uncertainty, has been applied to the constants of Tables 3 and 4 to minimize the number of digits required to reproduce the data accurately. The Dunham constants of ^{64}ZnD and ^{114}CdD are derived from those of ^{64}ZnH and ^{114}CdH using Eqs. (4) and (5), and require more digits, as determined by parameter sensitivities [53]. Complete lists of all the data used in our analyses, and the Dunham constants for all isotopologues are provided in the Supplementary data.

The equilibrium rotational constants ($B_e \approx Y_{0,1}$) of ^{64}ZnH and ^{114}CdH in Tables 3 and 4 have high precision, mainly because the pure rotational data were included in our data set. Using the B_e constants of ^{64}ZnH and

Table 3
Dunham and Born–Oppenheimer breakdown constants (in cm^{-1}) for the $X\,^2\Sigma^+$ ground state of ^{64}ZnH and ^{64}ZnD[a]

Dunham	^{64}ZnH	^{64}ZnD	Born–Oppenheimer breakdown	
$Y_{1,0}$	1603.1813(70)	1143.218719	$\delta^{H}_{1,0}$	1.1504(6)
$Y_{2,0}$	−50.50089(940)	−25.6614425		
$Y_{3,0}$	−1.5064(50)	−0.545649		
$Y_{4,0}$	−0.1612(9)	−0.04162259		
$Y_{0,1}$	6.69133166(1700)	3.402155578	$\delta^{H}_{0,1}$	0.0080074(62)
$Y_{1,1}$	−0.2825981(670)	−0.102371518	$\delta^{H}_{1,1}$	−0.000048(6)
$Y_{2,1}$	−0.0089738(860)	−0.002317077		
$Y_{3,1}$	−0.00113(5)	−0.0002079857		
$Y_{4,1}$	−0.0002689(81)	−0.0000352807		
$10^4 Y_{0,2}$	−4.648825(690)	−1.2028793	$10^4\,\delta^{H}_{0,2}$	−0.01962(21)
$10^4 Y_{1,2}$	−0.14087(220)	−0.02539308	$10^4\,\delta^{H}_{1,2}$	0.00582(15)
$10^4 Y_{2,2}$	−0.0191(17)	−0.00250599		
$10^4 Y_{3,2}$	−0.01801(37)	−0.001684422		
$10^9 Y_{0,3}$	10.804(220)	1.440468	$10^9\,\delta^{H}_{0,3}$	0.35(5)
$10^9 Y_{1,3}$	−8.66(66)	−0.809944		
$10^9 Y_{2,3}$	3.3(5)	0.22001		
$10^9 Y_{3,3}$	−2.02(8)	−0.096		
$10^{12} Y_{0,4}$	−3.19(20)	−0.212676	$\delta^{Zn}_{0,1}$	0.000141(2)
$10^{12} Y_{1,4}$	0.0(6)	0.0		
$10^{12} Y_{2,4}$	−3.0(3)	−0.101632		
$\gamma_{0,1}$	0.26258(4)	0.13342699		
$\gamma_{1,1}$	−0.019538(160)	−0.00707706		
$\gamma_{2,1}$	0.00182(25)	0.00046993		
$\gamma_{3,1}$	−0.001362(150)	−0.00025069		
$\gamma_{4,1}$	0.00021(3)	0.000027553		
$10^4\gamma_{0,2}$	−0.78782(110)	−0.2034188		
$10^4\gamma_{1,2}$	−0.005(2)	−0.00092		
$10^4\gamma_{2,2}$	−0.0120(9)	−0.0015744		
$10^9\gamma_{0,3}$	6.39(23)	0.8384		
$10^9\gamma_{1,3}$	−2.1(4)	−0.1964		

[a] The numbers in parentheses are 2σ uncertainties in the last quoted digits.

^{114}CdH, the associated equilibrium internuclear distances (r_e) of these species were determined to be 1.593478(2) and 1.760098(3) Å, respectively. The r_e distances of ^{64}ZnD and ^{114}CdD are expected to be slightly different from those of ^{64}ZnH and ^{114}CdH, respectively, due to the existence of $\delta^{H}_{0,1}$ correction parameters. Using the derived B_e constants in Tables 3 and 4, r_e distances of 1.593001(2) and 1.759695(2) Å were obtained for ^{64}ZnD and ^{114}CdD, respectively.

4. Discussion

The new Dunham constants for ZnH and CdH are compared with those determined from the diode laser infrared spectra [44,45] in Table 5. While the constants reported in [45] are in the form of mass-independent Dunham-type coefficients ($U_{l,m}$ and $\Delta_{l,m}$) formulated by Bunker [55] and Watson [56], it is straightforward to transform them to regular Dunham ($Y_{l,m}$) constants [54]. We compare only the B_e constants and the $Y_{l,0}$ coefficients that represent the vibrational energy. There is no point in comparing higher order $Y_{l,m}$ constants with $m > 0$, because our data set was much more extensive than the diode laser infrared data alone. It is interesting to note that although the $Y_{1,0}$ and $Y_{2,0}$ coefficients have very small relative uncertainties, their values depend strongly on the model, i.e., on the order of polynomial used for vibrational energy, see Table 5. In the ZnH/ZnD multi-isotopologue fits, our $Y_{l,0}$ constants are clearly preferred to those reported in diode laser infrared studies [44,45] because there was an extra vibration–rotation band in our data set, i.e., the new $v = 3 \rightarrow 2$ band of ZnD, which allowed us to determine higher order Dunham coefficients. In the CdH/CdD fits, the vibrational range of the data set used in our fit was the same as that used in the diode laser infrared studies, i.e., $v = 0$ to 2 for both CdH and CdD, but we used a different model. Instead of fitting the vibrational energies of CdH and CdD to two Dunham constants ($Y_{1,0}$ and $Y_{2,0}$) and introducing two Born–Oppenheimer breakdown correction parameters ($\delta^{H}_{1,0}$ and $\delta^{H}_{2,0}$), we used a third-order polynomial for $Y_{l,0}$ and only one correction parameter $\delta^{H}_{1,0}$. Our $Y_{1,0}$ and $Y_{2,0}$ coefficients are therefore considerably different from those of Urban et al. [44] and Birk et al. [45]. Fortunately, it is possible to ascertain which model is more reliable in this case, because the $v = 3 \rightarrow 2$ vibrational interval of ^{114}CdD is known with relatively high accuracy ($\pm 0.05\ cm^{-1}$) from Balfour's work [27]. He studied the $A\,^2\Pi \rightarrow X\,^2\Sigma^+$ electronic spectrum of CdD and observed a vibrational energy difference of 849.93 cm^{-1} between the $v = 3$ and 2 levels of ^{114}CdD [27]. Somewhat surprisingly, our derived Dunham constants for ^{114}CdD (Table 4) predict the $v = 3 \rightarrow 2$ vibrational interval to be 849.927 cm^{-1}, equal to Balfour's measured value within

Table 4
Dunham and Born–Oppenheimer breakdown constants (in cm^{-1}) for the $X\,^2\Sigma^+$ ground state of ^{114}CdH and ^{114}CdD[a]

Dunham	^{114}CdH	^{114}CdD	Born–Oppenheimer breakdown	
$Y_{1,0}$	1443.47421(310)	1025.923761	$\delta^{H}_{1,0}$	1.0707(11)
$Y_{2,0}$	−48.3345(25)	−24.397623		
$Y_{3,0}$	−3.0301(6)	−1.0866568		
$Y_{0,1}$	5.4470743(180)	2.750760873	$\delta^{H}_{0,1}$	0.00500315(1300)
$Y_{1,1}$	−0. 23936712(5700)	−0.085773934	$\delta^{H}_{1,1}$	0.00038(2)
$Y_{2,1}$	−0.006349(50)	−0.001617655		
$Y_{3,1}$	−0.0031315(140)	−0.000566863		
$10^4 Y_{0,2}$	−3.085445(650)	−0.78711618	$10^4\ \delta^{H}_{0,2}$	−0.00769(19)
$10^4 Y_{1,2}$	−0.1604(24)	−0.02903555		
$10^4 Y_{2,2}$	−0.012(3)	−0.00154331		
$10^4 Y_{3,2}$	−0.02216(94)	−0.002024817		
$10^9 Y_{0,3}$	0.13(8)	0.045634	$10^9\ \delta^{H}_{0,3}$	0.45(3)
$10^9 Y_{1,3}$	−0.7(2)	−0.063961		
$10^9 Y_{2,3}$	−4.186(100)	−0.271744		
$10^{12} Y_{0,4}$	−0.56(8)	−0.036354	$\delta^{Cd}_{0,1}$	0.0000495(9)
$10^{12} Y_{1,4}$	−4.17(14)	−0.192328		
$\gamma_{0,1}$	0.6304422(330)	0.31822593		
$\gamma_{1,1}$	−0.055197(170)	−0.01979479		
$\gamma_{2,1}$	0.01053(31)	0.00268293		
$\gamma_{3,1}$	−0.007754(200)	−0.00140363		
$\gamma_{4,1}$	0.00139(4)	0.000178766		
$10^4\gamma_{0,2}$	−1.6891(8)	−0.430364		
$10^4\gamma_{1,2}$	−0.046(2)	−0.0083269		
$10^4\gamma_{2,2}$	−0.0244(7)	−0.0031381		
$10^9\gamma_{0,3}$	8.99(21)	1.15619		
$10^9\gamma_{1,3}$	−5.2(4)	−0.47514		

[a] The numbers in parentheses are 2σ uncertainties in the last quoted digits.

Table 5
A comparison of the new Dunham constants of ZnH, ZnD, CdH, and CdD with those obtained in previous studies (all values are in cm^{-1}, and all uncertainties are 2σ)

Constant	^{64}ZnH		^{64}ZnD	
	This work	[45][a]	This work	[45][a]
$Y_{1,0}$	1603.181(7)	1615.748(23)	1143.219(5)	1147.398(12)
$Y_{2,0}$	−50.501(9)	−59.636(12)	−25.661(5)	−28.736(5)
$Y_{3,0}$	−1.506(5)	—	−0.546(2)	—
$Y_{4,0}$	−0.1612(9)	—	−0.0416(2)	—
$Y_{0,1}$	6.69133(2)	6.68686(33)	3.402156(7)	3.401588(136)
	^{114}CdH		^{114}CdD	
	This work	[45][a]	This work	[45][a]
$Y_{1,0}$	1443.474(3)	1460.945(8)	1025.924(2)	1032.200(4)
$Y_{2,0}$	−48.334(3)	−61.994(5)	−24.398(1)	−29.298(2)
$Y_{3,0}$	−3.0301(6)	—	−1.0867(2)	—
$Y_{0,1}$	5.44707(2)	5.44073(18)	2.750761(6)	2.749767(69)

[a] The $U_{l,m}$ and $\Delta_{l,m}$ constants reported in [45] were used to calculate these Dunham coefficients, and the uncertainties were obtained by propagation of errors.

its experimental uncertainty. On the other hand, using the CdD Dunham constants reported by Birk et al. [45] one predicts 856.413 cm^{-1} for the $v = 3 \rightarrow 2$ vibrational interval, which differs from the observed value by more than 6 cm^{-1}. This indicates that a second-order polynomial is inadequate for representing the vibrational energy levels of CdH or CdD, and proves that our third-order polynomial for $Y_{l,0}$ coefficients with only one correction parameter ($\delta^{H}_{1,0}$) is a more realistic model for those vibrational energies.

As for other diatomic hydrides studied by our group [57–59], several Born–Oppenheimer breakdown correction parameters for the hydrogen atom ($\delta^{H}_{l,m}$) were required in the multi-isotopologue fits for ZnH and CdH. Due to the presence of high quality rotational data (uncertainties $< 10^{-5}$ cm^{-1}), small correction parameters due to zinc and cadmium isotopes could be determined for the B_e constants (see the $\delta^{Zn}_{0,1}$ and $\delta^{Cd}_{0,1}$ values in Tables 3 and 4). The presence of these small correction parameters implies that the equilibrium internuclear distances (r_e) are not exactly

the same, even within different isotopes of zinc and cadmium.

In a previous study, Varberg and Roberts [48] reported that four Born–Oppenheimer breakdown correction parameters for $\gamma_{l,m}$ constants were required to fit all the pure rotation data in the $v = 0$ of CdH and CdD together. It is now clear that these correction parameters only appeared to be required because the vibrational dependence of the γ, γ_D, and γ_H constants had been overlooked. The $v = 0$ ground state of CdD lies more than 200 cm^{-1} lower than that of CdH, and the reduced mass scaling ratio in Eq. (5), derived by Brown and Watson [50], applies only to the equilibrium $\gamma_{l,m}$ constants associated with the bottom of the potential well, and not to the effective γ values at $v = 0$. The present work shows that when the vibrational dependence of the spin–rotation interaction constants is taken into account properly, no Born–Oppenheimer breakdown correction parameter is required for the $\gamma_{l,m}$ constants, and Eq. (5) accounts fully for the isotopologue dependence of these parameters. For each individual vibrational level, the γ_v constant is calculated from the following equation in which the $\gamma_{l,m}$ constants of different isotopologues are related by Eq. (5)

$$\gamma_v = \gamma_{0,1} + \gamma_{1,1}(v+1/2) + \gamma_{2,1}(v+1/2)^2 + \gamma_{3,1}(v+1/2)^3 + \gamma_{4,1}(v+1/2)^4. \quad (6)$$

If one plots $\gamma_v^{\alpha}(\mu_\alpha/\mu_1)$ versus $(v+1/2)\sqrt{(\mu_1/\mu_\alpha)}$ for different isotopologues, all the points should fall on a single curve, providing Eq. (5) holds exactly. This is in fact the case for ZnH/ZnD and CdH/CdD isotopologues, as is illustrated in Figs. 5 and 6. The individual γ_v constants are taken from Tables 1 and 2 (independent fits) and the solid curves are calculated from the $\gamma_{l,m}$ constants of Tables 3 and 4 (multi-isotopologue fits). The plots of Figs. 5 and 6 provide further confirmation for Eq. (5), which was derived by Brown and Watson [50]. Thus, the Born–Oppenheimer breakdown correction parameters for the spin–rotation interaction constants reported by Varberg and Roberts [48] were artifacts of their neglect of the vibrational dependence of γ.

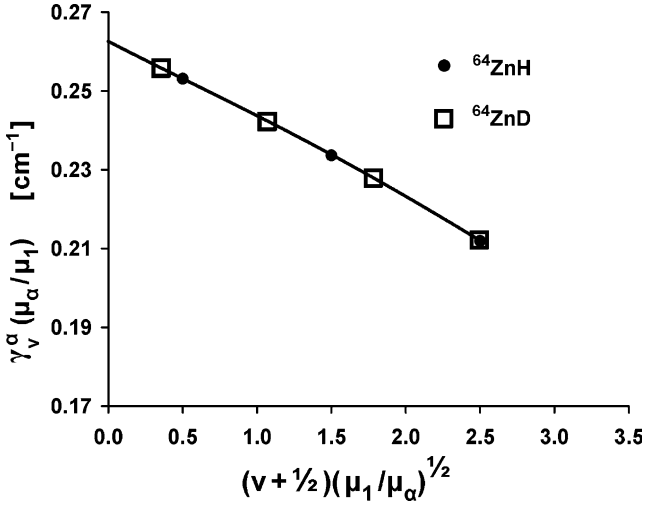

Fig. 5. The γ_v constants of ^{64}ZnH and ^{64}ZnD (from Table 1) are scaled by reduced masses and plotted versus the reduced mass scaled vibrational quantum numbers. The reference isotopologue ($\alpha = 1$) is ^{64}ZnH, and the solid curve is calculated from Eq. (6) using the constants of Table 3.

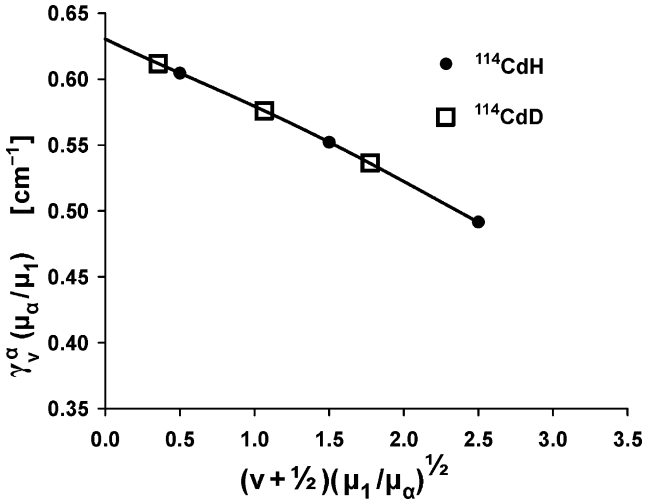

Fig. 6. The γ_v constants of ^{114}CdH and ^{114}CdD (from Table 2) are scaled by reduced masses and plotted versus the reduced mass scaled vibrational quantum numbers. The reference isotopologue ($\alpha = 1$) is ^{114}CdH, and the solid curve is calculated from Eq. (6) using the constants of Table 4.

Table 6
A comparison of the metal–hydrogen internuclear distances in MH and MH_2 molecules (M = Zn, Cd, Be, and Mg)

Metal	r_e(M–H)/Å	r_e(H–M–H)/Å	Δr_e/Å
^{64}Zn	1.593478(2)	1.52413(2)[a]	0.069
^{114}Cd	1.760098(3)	[1.67528][b]	0.085
^{9}Be	1.342436(2)[c]	1.326407(6)[d]	0.016
^{24}Mg	1.729721(1)[e]	[1.69841][f]	0.031

The numbers in parentheses are 2σ uncertainties in the last quoted digits.
[a] From [4].
[b] Experimental r_e is not available for CdH_2. The r_s structure from [3] is reported in brackets.
[c] From [57].
[d] From [60].
[e] From [59].
[f] Experimental r_e is not available for MgH_2. The r_s structure (in brackets) was calculated from the rotational constants of MgH_2 and MgD_2 reported in [61] and [62].

The metal–hydrogen internuclear distances (r_e) of ZnH, CdH, BeH, and MgH are compared in Table 6. All these molecules have a $^2\Sigma^+$ ground state with an unpaired electron in a non-bonding molecular orbital. The metal–hydrogen distances of MH_2 molecules (M = Zn, Cd, Be, and Mg) are thus expected to be very close to those of the corresponding MH molecules. We found that the M–H distances in ZnH and CdH are about 5% larger than those in ZnH_2 [4] and CdH_2 [3], respectively, while these differences are about 2% for BeH/BeH_2 and MgH/MgH_2 pairs (Table 6).

5. Conclusions

High resolution infrared emission spectra of ZnH, ZnD, CdH, and CdD were recorded with a Fourier transform

spectrometer, and a few vibration–rotation bands in the $X\ ^2\Sigma^+$ ground state were observed for these species. In addition, new measurements of pure rotational transitions in the $v = 1$ level of the $X\ ^2\Sigma^+$ ground state were obtained for CdH and CdD. The new data were combined with the previous data from diode laser infrared spectra and pure rotational spectra of ZnH/ZnD and CdH/CdD available in the literature. Empirical Dunham constants and Born–Oppenheimer breakdown correction parameters were obtained simultaneously from multi-isotopologue fits to the data, and the equilibrium metal–hydrogen internuclear distances were calculated. The reduced mass scaling ratio for the spin–rotation interaction constants derived by Brown and Watson [50] was further confirmed, as all isotopic data could be fitted together without any mass-scaled correction parameters for the $\gamma_{l,m}$ constants. Many of the Born–Oppenheimer breakdown parameters reported previously for CdH and CdD vanished when the vibrational dependences of the rotational and spin–rotation interaction constants were taken into account properly.

Acknowledgments

Funding for this work was provided in part by the Natural Sciences and Engineering Research Council (NSERC) of Canada. T.D.V. acknowledges support from the National Science Foundation in the form of a Research at Undergraduate Institutions award (# CHE-0518198) and from the Dreyfus Foundation in the form of a Henry Dreyfus Teacher-Scholar Award.

Appendix A. Supplementary data

Supplementary data for this article are available on ScienceDirect (www.sciencedirect.com) and as part of the Ohio State University Molecular Spectroscopy Archives (http://msa.lib.ohio-state.edu/jmsa_hp.htm).

References

[1] A. Shayesteh, D.R.T. Appadoo, I.E. Gordon, P.F. Bernath, J. Am. Chem. Soc. 126 (2004) 14356–14357.
[2] A. Shayesteh, S. Yu, P.F. Bernath, Chem. Eur. J. 11 (2005) 4709–4712.
[3] S. Yu, A. Shayesteh, P.F. Bernath, J. Chem. Phys. 122 (2005) 194301:1–6.
[4] A. Shayesteh, I.E. Gordon, D.R.T. Appadoo, P.F. Bernath, Phys. Chem. Chem. Phys. 7 (2005) 3132–3142.
[5] A. Shayesteh, S. Yu, P.F. Bernath, J. Phys. Chem. A 109 (2005) 10280–10286.
[6] E. Hulthén, Z. Phys. 11 (1922) 284–293.
[7] A. Kratzer, Ann. Physik. 71 (1923) 72–103.
[8] R.S. Mulliken, Nature 113 (1924) 489–490.
[9] E. Hulthén, Nature 116 (1925) 642.
[10] R.S. Mulliken, Proc. Natl. Acad. Sci. USA 12 (1926) 151–158.
[11] E. Hulthén, Z. Phys. 45 (1927) 331–336.
[12] R.S. Mulliken, Phys. Rev. 32 (1928) 388–416.
[13] W.W. Watson, Phys. Rev. 36 (1930) 1134–1143.
[14] E. Svensson, Z. Phys. 59 (1930) 333–352.
[15] E. Svensson, Nature 131 (1933) 28.
[16] G. Stenvinkel, E. Svensson, Nature 135 (1935) 955.
[17] G. Stenvinkel, Doctoral Dissertation, University of Stockholm (1936).
[18] E. Svensson, Doctoral Dissertation, University of Stockholm (1935).
[19] Y. Fujioka, Y. Tanaka, Sci. Pap. Inst. Phys. Chem. Res. 32 (1937) 143–156.
[20] O. Deile, Z. Phys. 106 (1937) 405–417.
[21] G. Stenvinkel, E. Svensson, E. Olsson, Ark. Mat. Astr. Fys. 26 A (1938) 1–15.
[22] S. Mrozowski, Phys. Rev. 58 (1940) 597–599.
[23] M.A. Khan, Proc. Phys. Soc. 80 (1962) 599–607.
[24] M.A. Khan, Proc. Phys. Soc. 80 (1962) 1264–1268.
[25] K.P. Huber, G. Herzberg, Molecular Spectra and Molecular Structure IV. Constants of Diatomic Molecules, Van Nostrand, New York, 1979.
[26] W.J. Balfour, A.W. Taylor, J. Mol. Spectrosc. 91 (1982) 9–21.
[27] W.J. Balfour, Phys. Scr. 25 (1982) 257–267.
[28] W.J. Balfour, K.S. Chandrasekhar, B. Lindgren, J. Mol. Spectrosc. 119 (1986) 126–136.
[29] W.J. Balfour, R.S. Ram, J. Mol. Spectrosc. 121 (1987) 199–208.
[30] L.C. O'Brien, W.T.M.L. Fernando, P.F. Bernath, J. Mol. Spectrosc. 139 (1990) 424–431.
[31] D.P. Chong, S.R. Langhoff, J. Chem. Phys. 84 (1986) 5606–5610.
[32] D.P. Chong, S.R. Langhoff, C.W. Bauschilcher Jr., S.P. Walch, H. Partridge, J. Chem. Phys. 85 (1986) 2850–2860.
[33] K. Balasubramanian, J. Chem. Phys. 93 (1990) 8061–8072.
[34] Ch. Jamorski, A. Dargelos, Ch. Teichteil, J.P. Daudey, J. Chem. Phys. 100 (1994) 917–925.
[35] E. Eliav, U. Kaldor, B.A. Hess, J. Chem. Phys. 108 (1998) 3409–3415.
[36] J. Dufayard, O. Nedelec, J. Physique 38 (1977) 449–458.
[37] X. Qing Tan, T.M. Cerny, J.M. Williamson, T.A. Miller, J. Chem. Phys. 101 (1994) 6396–6404.
[38] L.B. Knight Jr., W. Weltner Jr., J. Chem. Phys. 55 (1971) 2061–2070.
[39] E. Karakyriakos, J.R. Davis, C.J. Wilson, S.A. Yates, A.J. McKinley, L.B. Knight Jr., R. Babb, D.J. Tyler, J. Chem. Phys. 110 (1999) 3398–3410.
[40] A.J. McKinley, E. Karakyriakos, L.B. Knight Jr., R. Babb, A. Williams, J. Phys. Chem. A 104 (2000) 3528–3536.
[41] T.M. Greene, W. Brown, L. Andrews, A.J. Downs, G.V. Chertihin, N. Runeberg, P. Pyykkö, J. Phys. Chem. 99 (1995) 7925–7934.
[42] X. Wang, L. Andrews, J. Phys. Chem. A 108 (2004) 11006–11013.
[43] R.S. Wojslaw, B.F. Peery Jr., Astrophys. J. Suppl. Ser. 31 (1976) 75–92.
[44] R.-D. Urban, U. Magg, H. Birk, H. Jones, J. Chem. Phys. 92 (1990) 14–21.
[45] H. Birk, R.-D. Urban, P. Polomsky, H. Jones, J. Chem. Phys. 94 (1991) 5435–5442.
[46] M. Goto, K. Namiki, S. Saito, J. Mol. Spectrosc. 173 (1995) 585–590.
[47] F.A. Tezcan, T.D. Varberg, F. Stroh, K.M. Evenson, J. Mol. Spectrosc. 185 (1997) 290–295.
[48] T.D. Varberg, J.C. Roberts, J. Mol. Spectrosc. 223 (2004) 1–8.
[49] J.L. Dunham, Phys. Rev. 41 (1932) 721–731.
[50] J.M. Brown, J.K.G. Watson, J. Mol. Spectrosc. 65 (1977) 65–74.
[51] A.G. Maki, J.S. Wells, Wavenumber Calibration Tables from Heterodyne Frequency Measurements, NIST Special Publication 821, U.S. Government Printing Office, Washington (1991).
[52] R.J. Le Roy, DParFit 3.0, A Computer Program for Fitting Multi-Isotopomer Diatomic Molecule Spectra, University of Waterloo Chemical Physics Research Report CP-658 (2004); http://leroy.uwaterloo.ca.
[53] R.J. Le Roy, J. Mol. Spectrosc. 191 (1988) 223–231.
[54] R.J. Le Roy, J. Mol. Spectrosc. 194 (1999) 189–196.
[55] P.R. Bunker, J. Mol. Spectrosc. 68 (1977) 367–371.
[56] J.K.G. Watson, J. Mol. Spectrosc. 80 (1980) 411–421.
[57] A. Shayesteh, K. Tereszchuk, P.F. Bernath, R. Colin, J. Chem. Phys. 118 (2003) 1158–1161.
[58] A. Shayesteh, K.A. Walker, I. Gordon, D.R.T. Appadoo, P.F. Bernath, J. Mol. Struct. 695–696 (2004) 23–37.

[59] A. Shayesteh, D.R.T. Appadoo, I. Gordon, R.J. Le Roy, P.F. Bernath, J. Chem. Phys. 120 (2004) 10002–10008.
[60] A. Shayesteh, K. Tereszchuk, P.F. Bernath, R. Colin, J. Chem. Phys. 118 (2003) 3622–3627.
[61] A. Shayesteh, D.R.T. Appadoo, I. Gordon, P.F. Bernath, J. Chem. Phys. 119 (2003) 7785–7788.
[62] A. Shayesteh, D.R.T. Appadoo, I. Gordon, P.F. Bernath, Can. J. Chem. 82 (2004) 947–950.